Supporting Information

A stable amino-functionalized fluorinated metal-organic framework for efficient separation of propyne/propylene

Yun-Tao Huang[a], Zi-Meng Song[a], Xin-Ye Zhao[a], Beibei Li[b], Zhengyi Di*[a], Cheng-Peng Li*[a]

[a]Academy of Interdisciplinary Studies on Intelligent Molecules, Tianjin Key Laboratory of Structure and Performance for Functional Molecules, College of Chemistry, Tianjin Normal University, Tianjin, 300387 (China)
[b]Henan Key Laboratory of Polyoxometalate, College of Chemistry and Molecular Sciences, Henan University, Kaifeng, Henan 475004, China.

Materials and Instrumentation

The reagents and solvents used in the study were purchased commercially without further purification. Single crystal diffraction data were obtained using a Bruker APEX-II QUAZAR single crystal diffractometer. PXRD patterns were obtained using a Haoyuan DX-2700BH X-ray power diffractometer. TGA data were obtained using an SDT Q600 thermal analyzer. Gas adsorption measurements were performed with ASAP 2020 V4.02 (V4.02 H). Breakthrough experiments were performed on a BSD-MAB instrument coupled with a gas BSD-mass mass spectrometry (TCD-Thermal Conductivity Detector, detection limit 1 ppm) from Beishide Co, Ltd.

Adsorption/desorption experiments

ASAP 2020 V4.02 (V4.02 H) was used for both activation and testing prior to gas adsorption. Fresh **TNU-DPA-1** samples were subjected to reagent exchange with anhydrous methanol for 3 days, followed by vacuum drying at 353 K for 10 hours to remove solvent molecules from the material pores. The activated samples were subjected to gas adsorption in liquid nitrogen, ice-water bath and water bath, respectively. N_2 adsorption isotherms at 77 K and C_3H_4, C_3H_6 adsorption isotherms at 273 K and 298 K were collected.

Column breakthrough experiments

Dynamic breakthrough experiments of C_3H_4/C_3H_6 (v/v,1/99) were carried out on a dynamic gas breakthrough apparatus, in which a gas chromatography (GC) detector was used to monitor the gas flow at the outlet of the packed column. Before the start of the breakthrough experiments, the **TNU-DPA-1** samples need to be packed tightly into a stainless-steel packed column of 180 mm length and 3 mm inner diameter. Afterwards, it was activated for 10 hours under He gas flow and 353 K. Then a gas mixture of C_3H_4/C_3H_6 was passed at the corresponding flow rate. The flow rates of the

gases used can all be regulated with a mass flow controller. For breakthrough cycling experiments, samples need to be desorbed for 30 min under activated conditions to achieve material regeneration.

Computational details

The binding sites for C_3H_6 and C_3H_4 in **TNU-DPA-1** were determined through classical molecular simulations. The single X-ray crystallographic structures were subject to geometry optimization through the CASTEP module implemented with the Materials Studio [1] program, using density functional theory (DFT) using the generalized gradient approximation (GGA) with the Perdew-Burke-Ernzerhof (PBE) functional and the double numerical plus d-functions (DNP) basis set. The energy, force, and displacement convergence criteria were set as 1×10^{-5} Ha, 2×10^{-3} Ha/Å and 5×10^{-3} Å, respectively. The calculated electrostatic potential for **TNU-DPA-1** was mapped onto the Connolly surface with a probe radius of 1.0 Å. Simulated annealing (SA) calculations [2] were performed for a single molecule of C_3H_6 and C_3H_4 through a canonical Monte Carlo (NVT) process, and all MOF atoms were kept fixed at their positions throughout the simulations. The initial configurations were further optimized to ensure a more efficient energy landscape scanning for every MOF- C_xH_x complex, and the optimized configuration having the lowest energy was used as the global minimum for the subsequent analysis and calculation. The static binding energy (at T= 0 K) was then calculated: $\triangle E = E_{MOF} + E_{gas} - E_{MOF+gas}$.

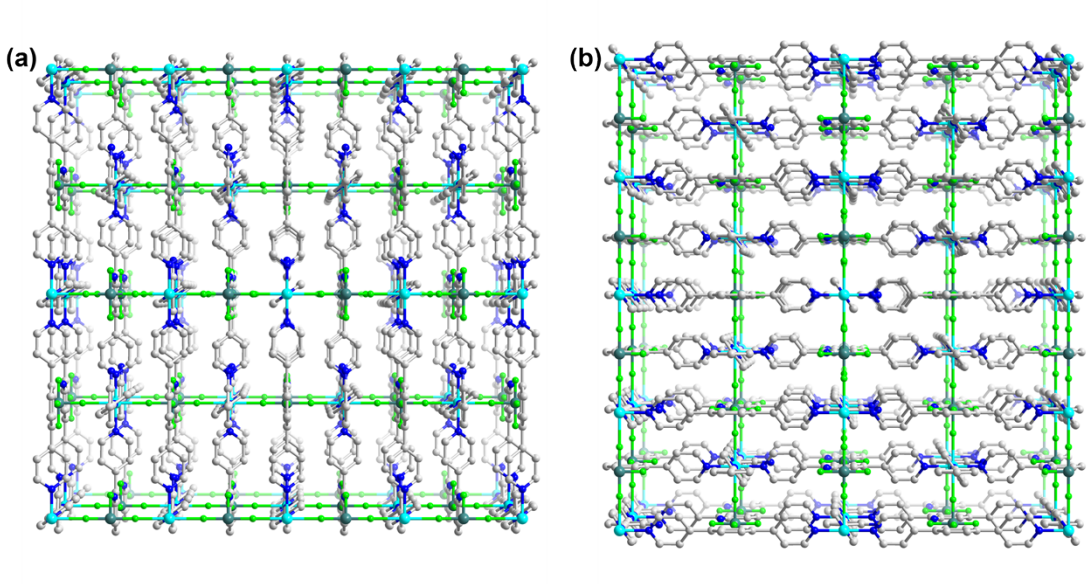

Figure S1. Stacking diagram of the **TNU-DPA-1** crystal structure in the (a) a-axis and (b) b-axis directions.

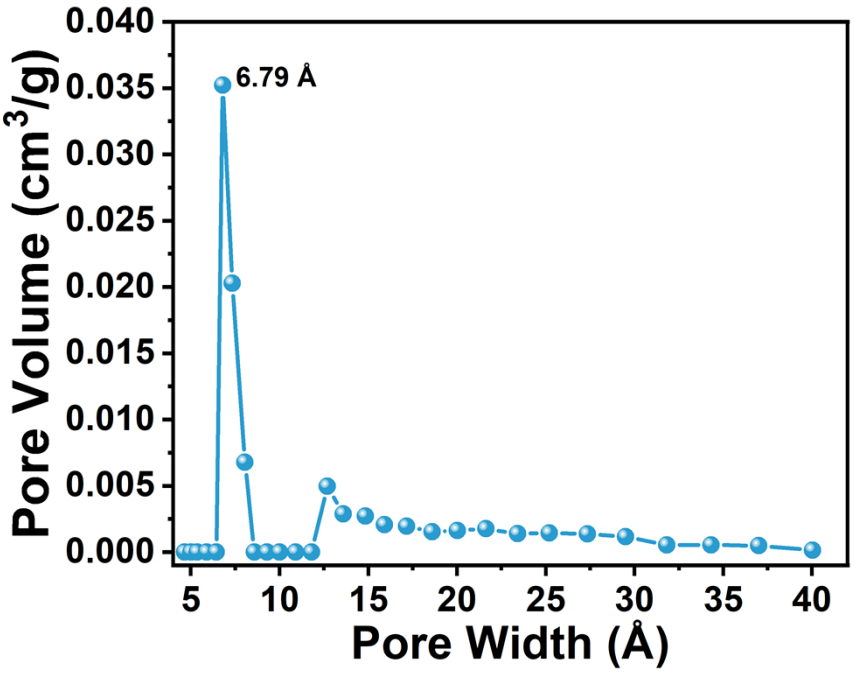

Figure S2. Pore size distribution of **TNU-DPA-1**.

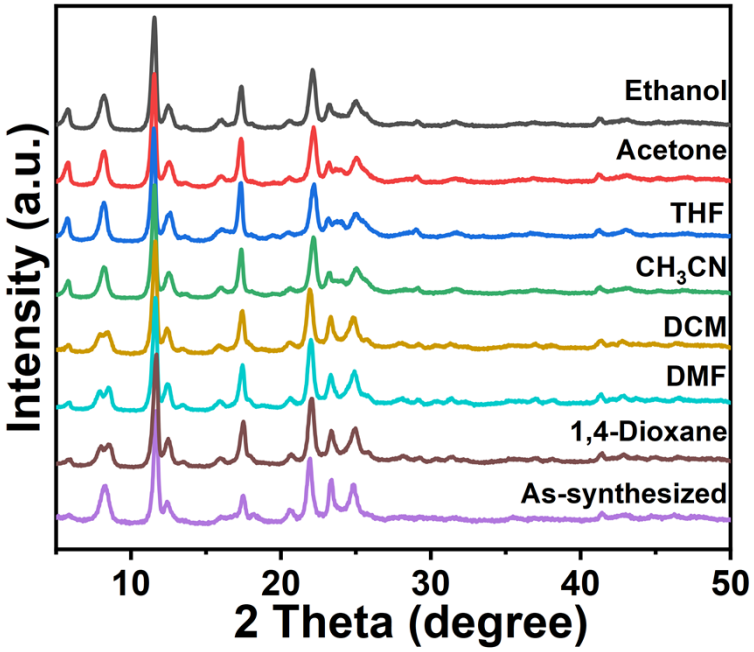

Figure S3. PXRD patterns of **TNU-DPA-1** samples after immersion in different solvents for 24 hours.

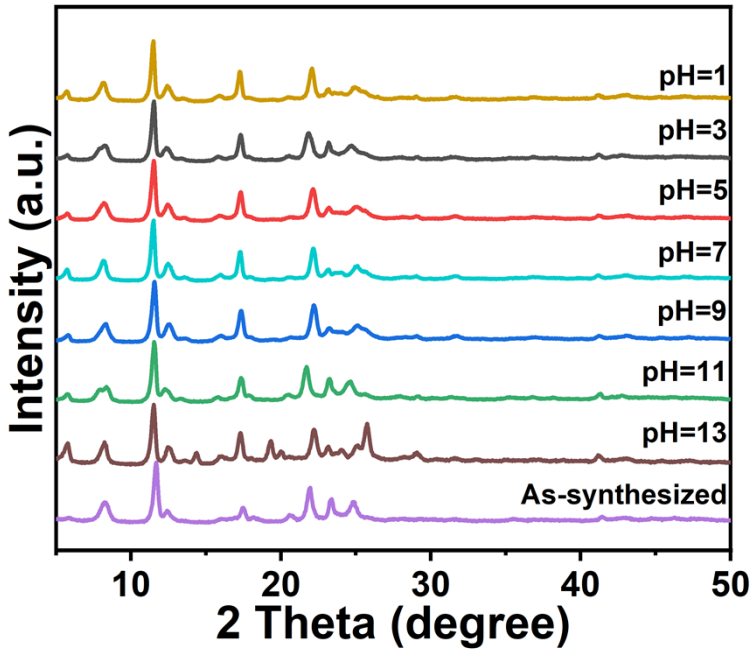

Figure S4. PXRD patterns of **TNU-DPA-1** samples after immersion in aqueous solutions of different pH values for 24 hours.

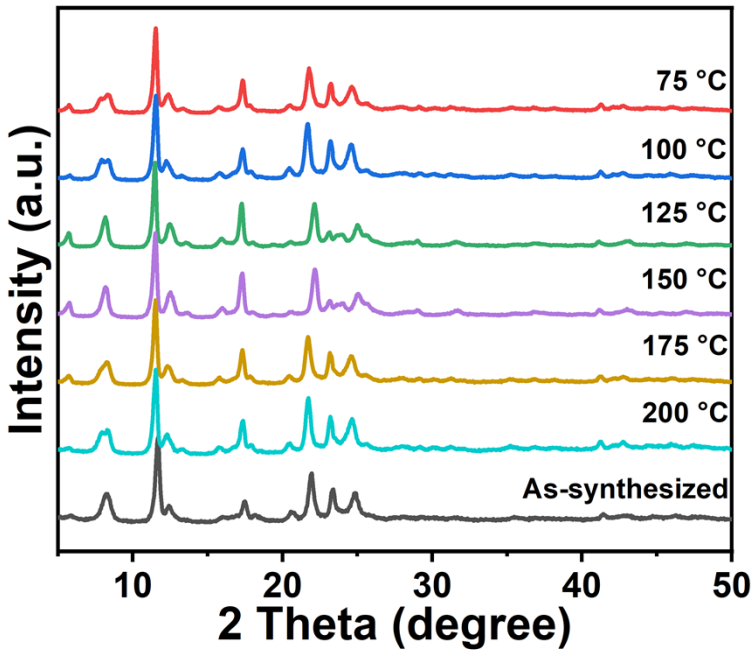

Figure S5. Variable temperature PXRD patterns of **TNU-DPA-1** samples.

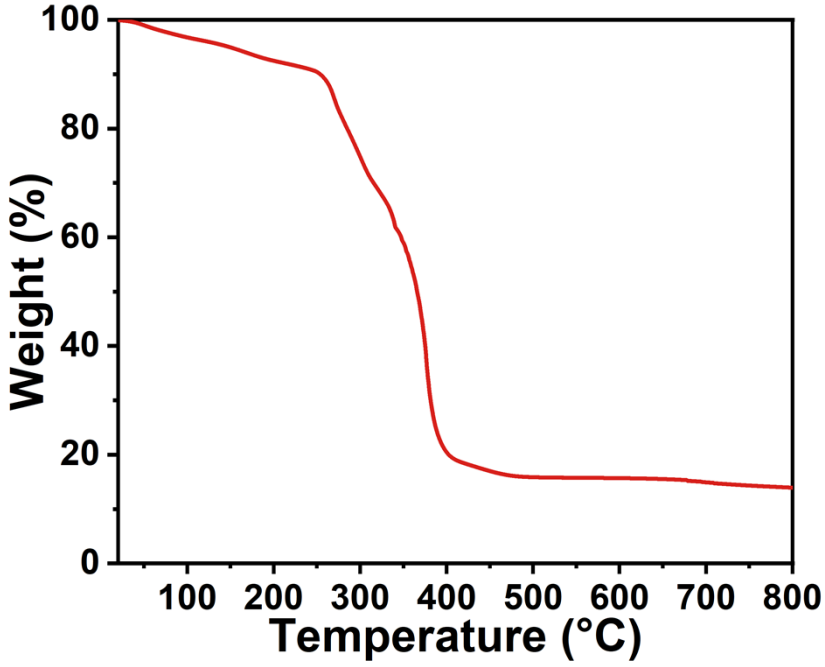

Figure S6. Thermogravimetric analysis of **TNU-DPA-1** under nitrogen atmosphere.

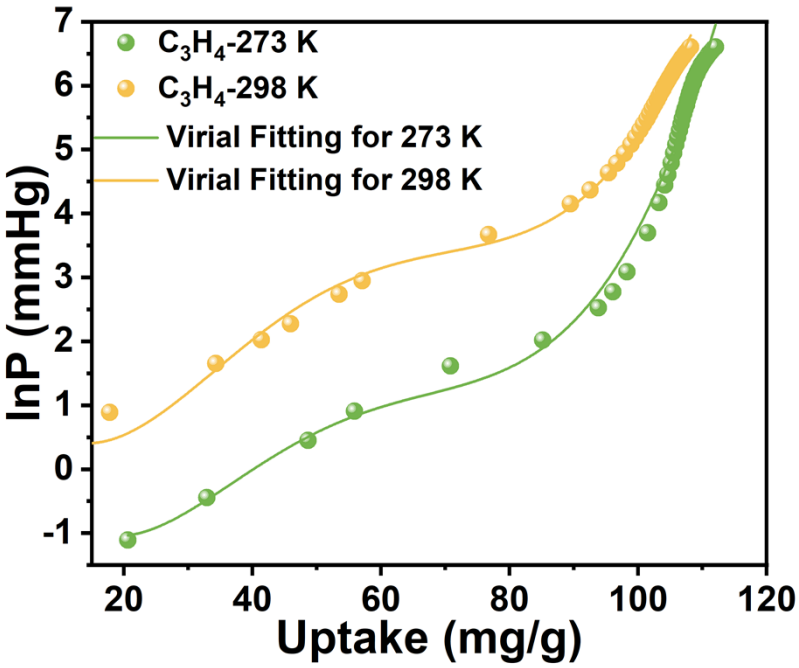

Figure S7. Virial fitting of C_3H_4 adsorption isotherms for **TNU-DPA-1** at 273 K and 298 K.

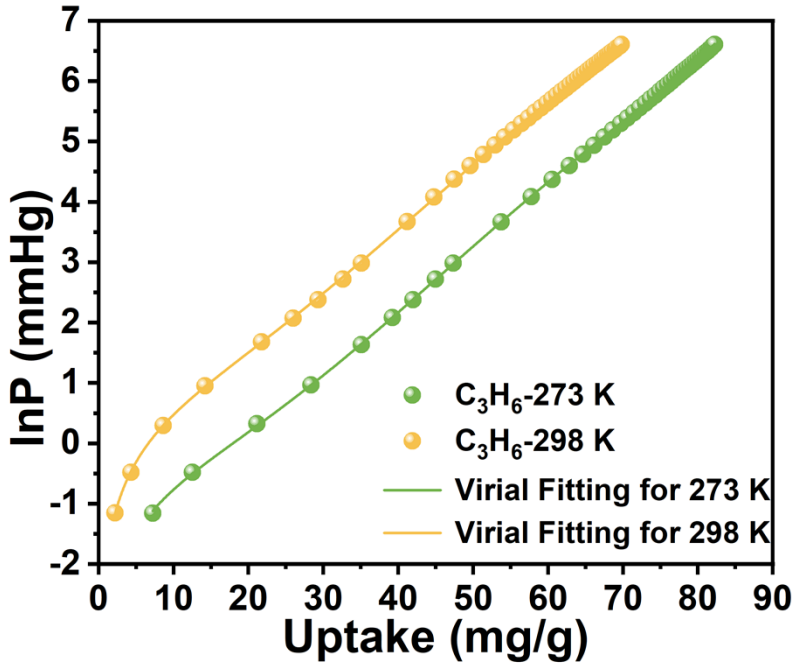

Figure S8. Virial fitting of C_3H_6 adsorption isotherms for **TNU-DPA-1** at 273 K and 298 K.

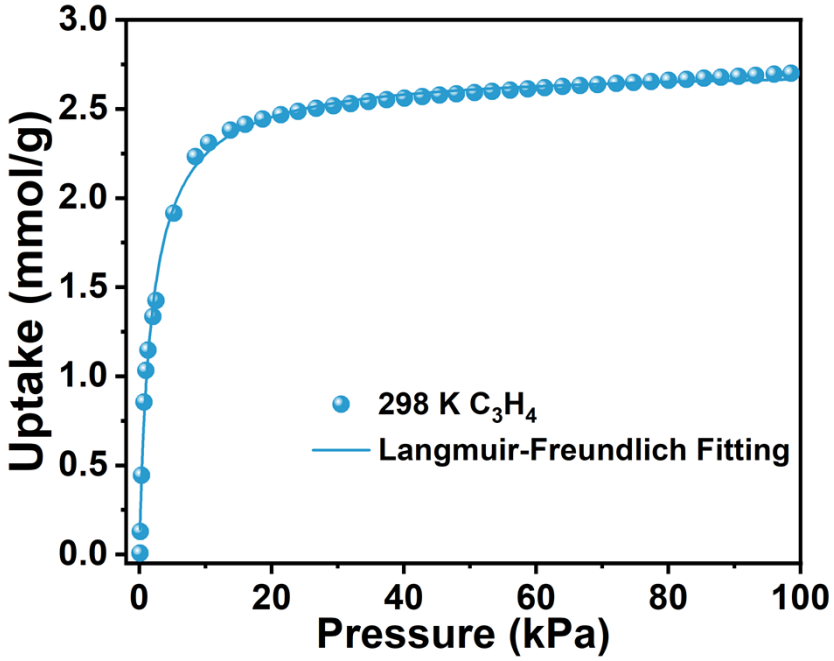

Figure S9. Langmuir-Freundlich fitting of C_3H_4 at 298 K.

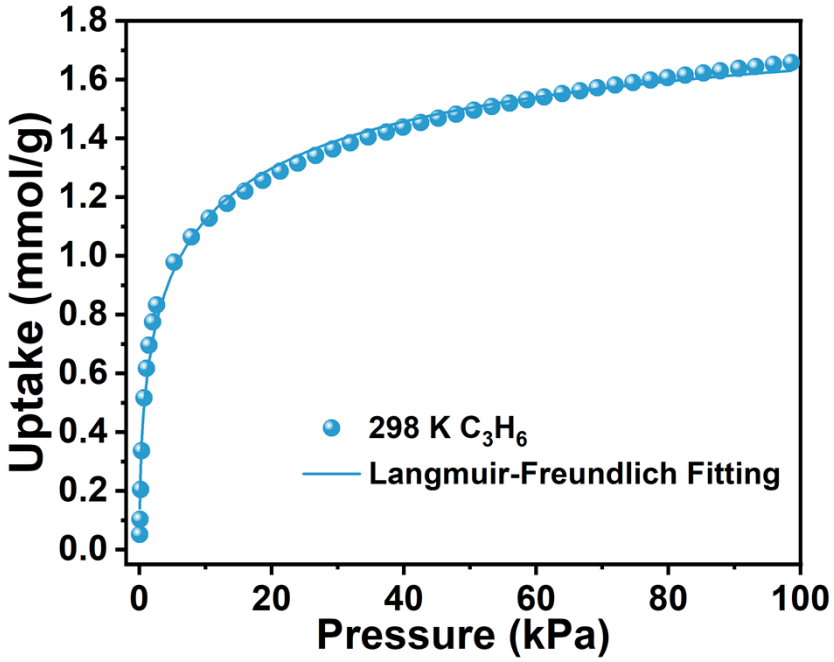

Figure S10. Langmuir-Freundlich fitting of C_3H_6 at 298 K.

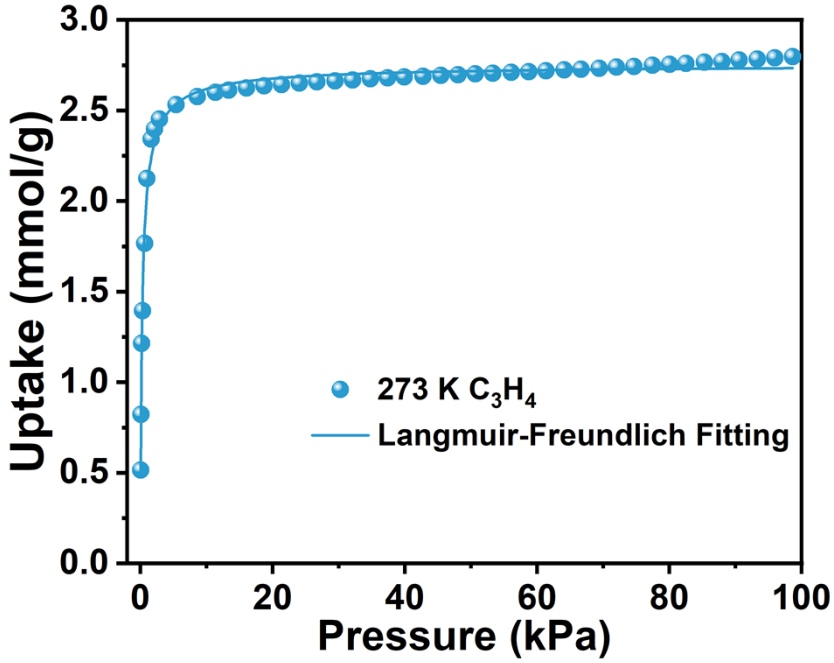

Figure S11. Langmuir-Freundlich fitting of C_3H_4 at 273 K.

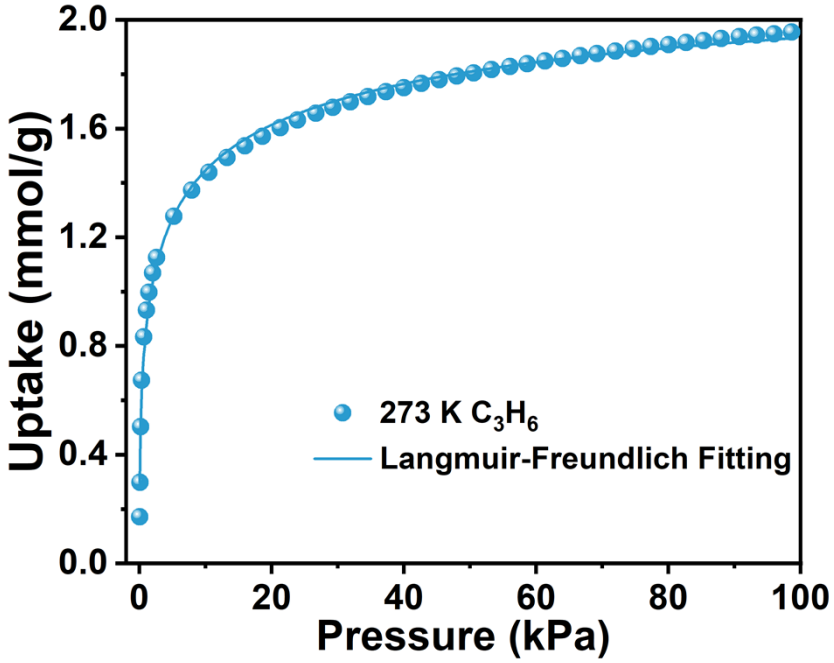

Figure S12. Langmuir-Freundlich fitting of C_3H_6 at 273 K.

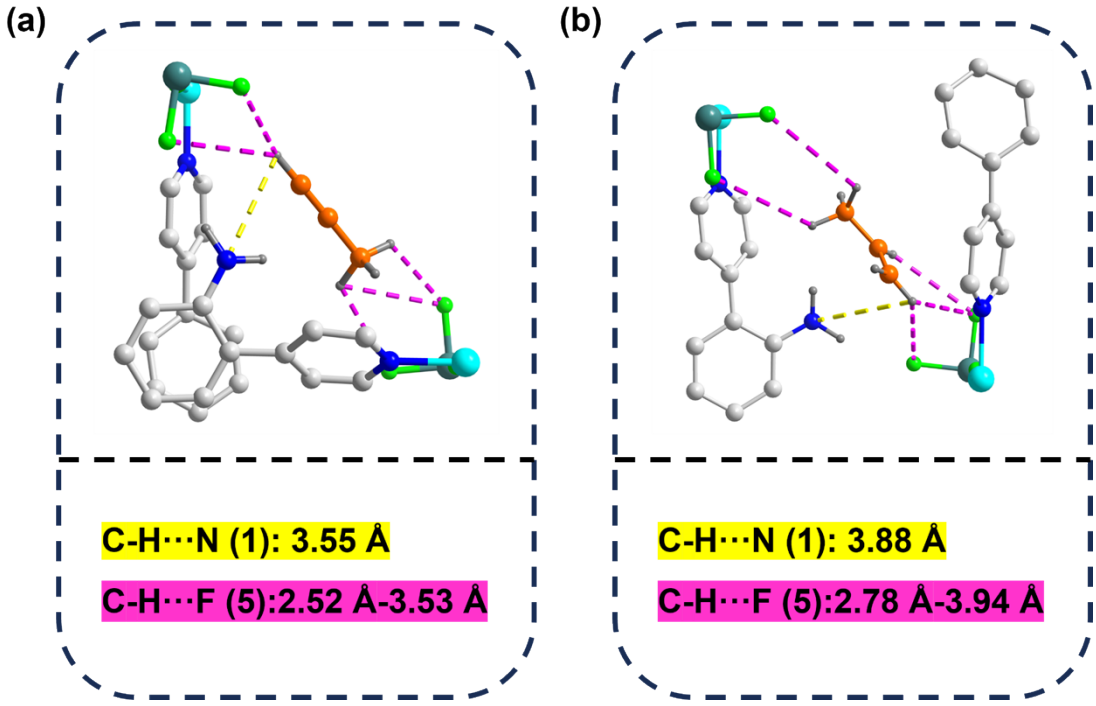

Figure S13. DFT-calculated interaction sites of **TNU-DPA-1** with the gas molecules (a) C_3H_4 and (b) C_3H_6.

Table S1. Crystal data and structure refinement for **TNU-DPA-1**

Complex	**TNU-DPA-1**
formula	$C_{32}H_{12}CuF_6N_8Si$
CCDC	2493666
T (K)	222
crystal system	tetragonal
space group	I4/mmm
a (Å)	15.391
b (Å)	15.391
c (Å)	8.068
α (deg)	90
β (deg)	90
γ (deg)	90
V (Å^3)	1911.1
Z	16
D_c (g/cm^3)	1.255
R_{int}	0.1177
F(000)	730
Goof	1.211
R_1, *w*R (I > 2σ(I))[a]	0.0644, 0.1868
R_1, *w*R (all date)[b]	0.0665, 0.1888

[a] $R = \sum||F_o| - |F_c||)/\sum|F_o|$. [b] $wR = |\sum w(F_o - F_c)^2/\sum w(F_o^2)^2|^{1/2}$

Table S2. Comparison of the C_3H_4/C_3H_6 separation properties of **TNU-DPA-1** and some superior MOF materials at 298 K and 100 kPa.

Sample	C_3H_4 uptake at 100 kPa (mmol/g)	C_3H_6 uptake at 100 kPa (mmol/g)	C_3H_4/C_3H_6 adsorption ratio	Selectivity C_3H_4/C_3H_6 (v/v,1/99)	C_3H_6 Productivity (mmol/g)
ELM-12	2.77	1.43	1.93	84	17
FJI-W1	7.09	6.27	1.13	2.2	52.9
JXNU-6a	5.07	3.57	1.42	3.1	8.9
ZJUT-1	2.24	0.84	2.67	70	9.8
SIFSIX-1-Cu	8.63	5.88	1.47	8.97	9.4
SIFSIX-2-Cu-i	3.77	2.63	1.43	30.58	25.9
SIFSIX-3-Ni	2.85	2.72	1.05	242.06	20.5
ZIF-8	6.27	4.07	1.54	1.9	1.3
Cu-BTC	10.47	8.33	1.26	3.2	6.3
UIO-66	10.23	3.33	3.07	15	0.9
Co-MOF-74	7.47	5.95	1.26	-	7.1
Mg-MOF-74	9.40	6.49	1.45	-	5.4
This work	**2.70**	**1.65**	**1.64**	**10.9**	**19.6**

Table S3. Comparison of **TNU-DPA-1** with fluorinated MOF materials possessing similar structures.

Sample	Gas mixtures	Uptake ($cm^3\ g^{-1}$)	Q_{st} ($kJ\ mol^{-1}$)	IAST Selectivity
TNU-DPA-1	C_3H_4/C_3H_6	60.49/37.14	42.5/31.3	10.9
SIFSIX-1-Cu	C_3H_4/C_3H_6	193.31/131.71	37/27	8.97
SIFSIX-2-Cu-i	C_3H_4/C_3H_6	84.45/58.91	45/37	30.58
SIFSIX-3-Ni	C_3H_4/C_3H_6	63.84/60.93	68/47	242.06
	C_2H_2/CO_2	73.92/60.48	36.7/50.9	7.7
SIFSIX-14-Cu-i	C_3H_4/C_3H_6	80.42/35.62	51/41	112.86
GeFSIX-14-Cu-i	C_3H_4/C_3H_6	75.26/33.6	-	306.12
TIFSIX-14-Cu-i	C_3H_4/C_3H_6	86.46/31.36	-	240.14
SIFSIX-3-Zn	C_3H_4/C_3H_6	50.62/40.32	-	115
ZU-16-Co	C_3H_4/C_3H_6	59.36/47.04	-	248
ZJUT-1	C_3H_4/C_3H_6	50.18/18.82	33.6/-	70
	C_2H_2/CO_2	73.92/51.52	44.2/40.2	11.7
ZU-62	C_3H_4/C_3H_6	81.31/59.81	71/52	46.31
TIFSIX-4-Cu-i	C_2H_2/C_2H_4	96.32/33.61	40.8/29.4	11
USTA-121	C_2H_2/CO_2	71.3/36.4	-	-
BSF-3	C_2H_2/C_2H_4	80.42/53.09	42.7/28.1	8.1

References

[1] Materials Studio v7.0, Biovia Software Inc., S.D., CA 92121, USA.
[2] Kirkpatrick, S.; Gelatt, C. D.; Vecchi, M. P., Optimization by Simulated Annealing. Science 1983, 220, 671.